High-spin states in the odd-odd nucleus ^{212}At

T. P. Sjoreen,* U. Garg,† and D. B. Fossan
Department of Physics, State University of New York, Stony Brook, New York 11794

J. R. Beene,‡ T. K. Alexander, E. D. Earle, O. Häusser, and A. B. McDonald
Nuclear Physics Branch, Atomic Energy of Canada Limited, Chalk River Laboratories, Chalk River, Ontario K0J1J0, Canada
(Received 5 February 1979)

The properties of high-spin states in ^{212}At, including three isomers, have been studied with the ^{208}Pb(^{7}Li,3n)^{212}At reaction. In-beam measurements with Ge(Li) and intrinsic Ge detectors of γ-ray excitation functions, γ-γ coincidences, γ-ray angular distributions, pulsed-beam-γ timing, and perturbed angular distributions with an applied magnetic field were made to establish a decay scheme, level energies, γ-ray multipolarities, spin-parity assignments, isomeric lifetimes, and g factors. High-spin states up to 15$\hbar$ were identified as predominantly three proton $[(\pi h_{9/2})^3$ or $(\pi h_{9/2})^2(\pi i_{13/2})]$ states of the (N = 126) ^{211}At nucleus coupled to a neutron in either the $g_{9/2}$, $i_{11/2}$, or $j_{15/2}$ orbitals. The experimental energy levels, g factors, and $B(M2)$ value are compared with shell model calculations.

[NUCLEAR REACTIONS ^{208}Pb(^{7}Li, 3n)^{212}At E =32–44 MeV; measured γ excitations, γ-γ coin, γ-$W(\theta)$, pulsed-beam-γ timing, perturbed angular distributions; deduced levels, γ multipolarities, J^π, $T_{1/2}$, $B(E1)$, $B(M2)$, g.]

I. INTRODUCTION

The study of odd-odd nuclei is most important for the determination of the effective proton-neutron residual interactions in different nuclear regions. Generally, these nuclei are difficult to study because of the high level densities involved. However, if the single particle levels available to the valence nucleons have large values of orbital angular momentum, then considerable structure information can be obtained from the yrast levels because these levels will generally involve high-spin configurations of a nearly pure nature. Moreover, some of these levels are frequently isomeric, allowing the nuclear wave functions to be probed by lifetime and g-factor measurements. Since heavy-ion fusion evaporation reactions preferentially populate yrast states, the utilization of these reactions combined with in-beam γ-ray methods offer an effective technique for studying the nuclear structure of odd-odd nuclei.

An interesting odd-odd nucleus in this respect is ^{212}At with three valence protons and one valence neutron outside the closed ^{208}Pb core (N= 126, Z = 82). The structure of the high-spin states is expected to involve the three protons in the $h_{9/2}$, $f_{7/2}$, and $i_{13/2}$ orbits coupled to the neutron in either the $g_{9/2}$, $i_{11/2}$, or $j_{15/2}$ orbit. In particular, it is expected that levels in ^{212}At should be identified as three-proton yrast levels in ^{211}At coupled to the odd neutron. The ^{212}At states involving seniority one ^{211}At states should be similar to ^{210}Bi yrast levels. The purpose of the present study is to determine experimentally the properties of high spin states in ^{212}At and to compare these results with ^{211}At and ^{210}Bi.

At the beginning of the present study the only available data on ^{212}At were from the studies[1] of the α decay of the ground state [$T_{1/2}$ = 0.315(3) sec] and the 225-keV metastable state [$T_{1/2}$ = 0.122(1) sec] to excited states in ^{208}Bi. These studies tentatively identified the spins and parities of the ground state and 225-keV state as (1^-) and (9^-), respectively. In the present study, high spin states in ^{212}At were investigated with in-beam γ-ray measurements via the ^{208}Pb(^{7}Li, 3n) fusion evaporation reaction. The features of fusion evaporation reactions that are useful to γ-ray spectroscopy will not be repeated here, but have been described in detail elsewhere.[2] To extract the desired experimental information, the following measurements were made: γ excitations, γ-γ coincidences, γ angular distributions, pulsed-beam-γ timing, and g-factor measurements. From these measurements the level scheme and electromagnetic properties were determined. Preliminary results of these measurements have been reported previously.[3]

The experimental procedure used in the present study is described briefly in Sec. II. For a more detailed description of the γ-γ coincidence, γ angular distribution, and pulsed-beam-γ measurements carried out at Stony Brook, see Ref. 4; for a detailed description of the g-factor measurements carried out at Chalk River, see Ref. 5. The experimental results for ^{212}At are presented in Sec. III and a comparison with conventional shell model calculations is discussed in Sec. IV.

II. EXPERIMENTAL PROCEDURE

The in-beam γ-ray measurements following the ^{208}Pb(^{7}Li, $3n$)^{212}At fusion evaporation reaction were carried out at both the Stony Brook and Chalk River tandem Van de Graaff accelerators. The γ-ray experiments at Stony Brook included γ-γ coincidence, γ angular distribution, and pulsed-beam-γ timing measurements at a typical beam energy of 33 MeV. The target was an isotopically enriched (99%) ^{208}Pb foil of 200 mg/cm^2 thickness. For these measurements, several large coaxial Ge(Li) detectors with energy resolutions of 2 keV full width at half maximum (FWHM) at 1.33 MeV were used. In addition, for γ rays with energies <150 keV, a 5 mm planar intrinsic Ge detector with an energy resolution of 0.5 keV FWHM at 122 keV was employed. The angular distribution measurements were made with a movable Ge(Li) detector positioned 11 cm from the target while another Ge(Li) detector placed at 90° to the beam served as a monitor; γ-ray singles spectra were taken at five angles between 0° and 90°. The function $W(\theta)=I_\gamma(1+A_2P_2+A_4P_4)$ was fitted to the data (normalized to include dead time and geometric effects) to obtain the relative γ-ray intensity I_γ and the Legendre polynominal coefficients A_2 and A_4. The γ-γ coincidence measurements were made with a standard fast-slow coincidence system and the data were stored on magnetic tape event by event for later off-line analysis. For the pulsed-beam-γ timing measurements, the ^{7}Li beam was pulsed with a repetition period of 1 μsec and a pulse width of about 3 nsec FWHM. Delayed γ-ray spectra were collected for several time windows from 30 to 400 nsec. To obtain more accurate lifetime results for the observed isomers, time differential measurements for the delayed γ rays were also made. The mean lifetime τ was extracted by fitting the function $B+Ae^{-t/\tau}$ to the Compton subtracted data; A is the amplitude at $t=0$ and B is a constant background. For cases involving isomers that were fed both directly and by a higher lying isomer of mean lifetime τ_1, the function $A_1[\tau_1/(\tau_1-\tau_2)](e^{-t/\tau_1}-e^{-t/\tau_2})+A_2e^{-t/\tau_2}+B$ was fitted to the data to obtain the mean lifetime τ_2 and the amplitudes A_1 and A_2 at $t=0$. Again B is a constant background.

The γ-ray experiments carried out at Chalk River included excitation functions and g-factor measurements. For these experiments a natural Pb target thick enough to stop the beam was used. The decay γ rays were detected by two large coaxial Ge(Li) detectors with energy resolutions of 2 keV FWHM at 1.33 MeV. The γ-excitation study was carried out for beam energies ranging from 34 to 44 MeV in increments of 2 MeV. The g factors were measured with the time differential perturbed angular distribution method[6] (TDPAD). For this measurements, the target was placed in a uniform magnetic field (2.29 T) which was applied perpendicular to the beam axis. The decay γ rays were detected by two Ge(Li) detectors positioned at ±135° to the beam. Data were accumulated at beam energies of 36 and 42 MeV using beam pulse repetition periods of 0.8 and 1.6 μsec, respectively. The total time resolution for the beam pulsing and the γ-ray detectors was less than 4 nsec FWHM. Data involving a single isomeric level were analyzed to form the standard ratio

$$R(t)=\frac{[N(+135°,t)-N(-135°,t)]}{[N(+135°,t)+N(-135°,t)]}$$

where $N(\theta,t)$ is the normalized yield after background subtraction. For γ rays with $A_4\approx 0$, the ratio data were fitted with

$$R(t)=[3A_2/(4+A_2)]\sin[2(\omega_Lt-\Delta\phi)],$$

where ω_L is the Larmor precession frequency and the phase $\Delta\phi$ accounts for any deviation from the symmetric detector position. The analysis of TDPAD data involving two isomeric levels is more complicated and is discussed in Ref. 7.

III. EXPERIMENTAL RESULTS

The γ-ray excitation measurements following the bombardment of ^{208}Pb with ^{7}Li were used to help identify γ rays originating from excited states in ^{212}At. The 184-, 278-, 377-, 479-, and 663-keV γ rays shown in Fig. 1 were observed to have a similar excitation function which is consistent with the cross section estimated for the (^{7}Li, $3n$) channel; this strongly suggests that these γ rays originate from the same nucleus, which is expected to be ^{212}At. Moreover, the excitation function of these γ rays differed considerably from the excitation functions of γ rays from ^{209,210}Bi, ^{210}Po, and ^{211}At, indicating that these γ rays did not originate from the (^{7}Li, $4n$)^{211}At fusion evaporation reaction or from the breakup reactions (^{7}Li, $\alpha 2n$)^{209}Bi, (^{7}Li, αn)^{210}Bi, and (^{7}Li, $t2n$)^{210}Po. The only remaining channels expected to be populated with significant strength were the (^{7}Li, $3n$)^{212}At, (^{7}Li, $2n$)^{213}At, and (^{7}Li, t)^{212}Po. However, a recent study[8] has identified the γ rays originating from ^{212}Po and ^{213}At. Since the 184-, 278-, 377-, 479-, and 663-keV γ rays were the only strong, unidentified lines left

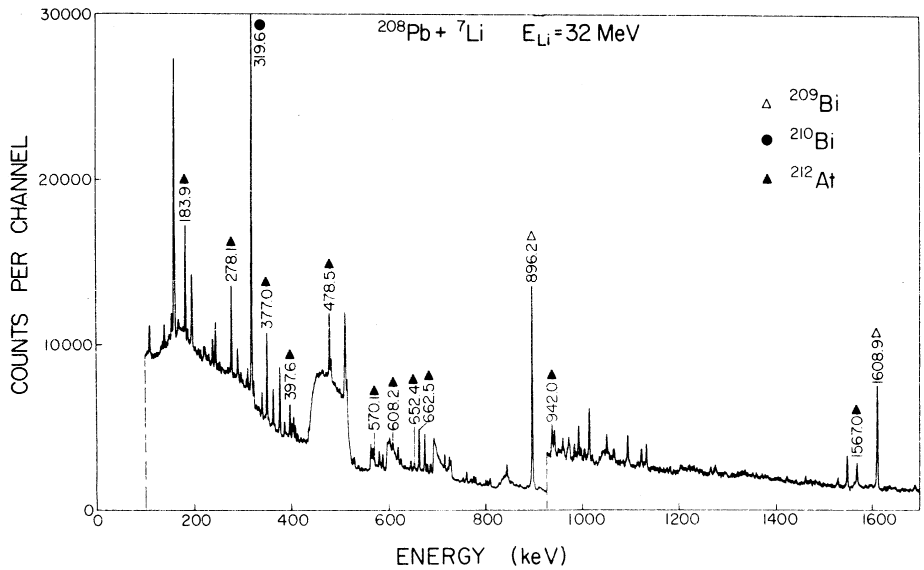

FIG. 1. The γ-ray spectrum observed with a Ge(Li) detector positioned 90° to the beam for the bombardment of a thick ^{208}Pb target with 32-MeV ^{7}Li ions. The Doppler broadened γ ray at 478 keV is from inelastic excitation of ^{7}Li.

in the ^{208}Pb + ^{7}Li spectrum, they were assigned to ^{212}At. This study[8] also showed, with a delayed γ-excitation measurement, that ^{212}At was being populated with much greater strength than either ^{212}Po or ^{213}At.

The results of the γ-γ coincidence measurement are summarized in Table I. From these results a level scheme for ^{212}At was constructed as shown in Fig. 6. The primary feature of this level scheme is the strong γ-ray cascade from the unobserved isomeric state at (1543 + Δ) keV to the isomeric state at 888 keV which subsequently decays via two cascades to the 225-keV metastable state. Coincidence spectra for four members of the γ-ray cascade are shown in Fig. 2. The evidence for the (1543 + Δ)-keV isomeric state and the assumption that the γ-ray cascade ends at the (9-) 225-keV metastable state will be discussed later. Also observed in coincidence with the above γ-ray cascade are the 608- and 570-keV γ rays. Assuming these γ rays are members of the stretched yrast cascade, they would then directly feed the (1543 + Δ)-keV unobserved isomeric level (see Fig. 6).

The 398-, 436-, 652-, and 942-keV γ rays were also assigned to ^{212}At on the basis of the γ-γ co-

TABLE I. Results of the γ-γ coincidence and angular distribution measurements for ^{212}At.

E_γ (keV) [a]	I_γ [b]	A_2	A_4	γ rays coincident with E_γ [c]
183.9	62	-0.13 ± 0.02		278.1, 377.0, 397.6, 436.0, 478.5, 942.0
278.1	62	-0.22 ± 0.01	-0.02 ± 0.02	183.9, 377.0, 478.5, (608.2), 662.5
377.0	70	-0.06 ± 0.01		183.9, 278.1, 478.5, 570.1, 608.2, 662.5
397.6	17 [d]			183.9, 478.5, 652.4, 662.5
436.0				183.9, 478.5, 662.5
478.5	98	0.00 ± 0.02		183.9, 278.1, 377.0, 436.0, (608.2)
570.1	18	0.29 ± 0.08	0.1 ± 0.1	278.1, (377.0)
608.2	23	0.09 ± 0.06	0.1 ± 0.1	278.1, 377.0
652.4	7 [d]			397.6
662.5	100	0.31 ± 0.02	-0.02 ± 0.02	278.1, 377.0, 397.6, 436.0, (608.2)
942.0	21 [d]			183.9, (478.5), (662.5)

[a] All γ-ray energies are accurate to 0.2 keV.
[b] γ-ray intensities are normalized to the 662.5-keV γ-ray yield and are accurate to 10%, unless otherwise noted.
[c] Parentheses around γ-ray energy indicate a weak coincidence.
[d] The γ-ray intensity is estimated from the γ-γ coincidence results and is only accurate to ±40%.

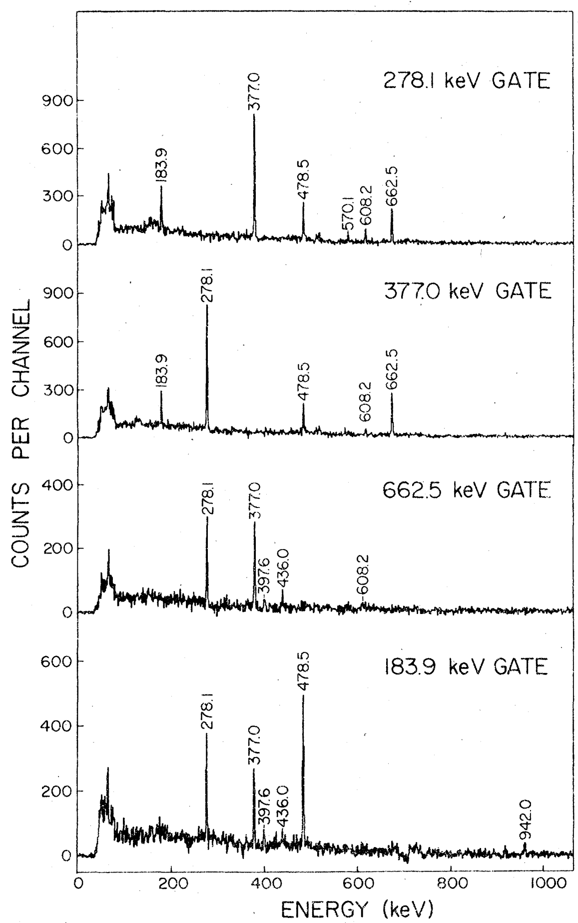

FIG. 2. γ-γ coincidence spectra from the $^{208}Pb(^{7}Li, 3n)$-^{212}At reaction observed with the two Ge(Li) detectors for four selected γ-ray gates.

incidence measurements. These γ rays, which were weaker in intensity, define levels at 1285, 1324, 1830, and 1938 keV (see Fig. 6).

The results obtained from the angular distribution measurements are also summarized in Table I. The relative γ-ray intensities are listed, as well as angular distribution A_2 and A_4 coefficients for those γ-ray transitions that could be isolated in the singles Ge(Li) spectra. An interpretation of these results in terms of γ-ray multipolarities, J^{π} assignments, and the level scheme will be given at the end of this section.

Evidence for three isomeric states in ^{212}At was found in the pulsed-beam-γ timing data. The delayed γ-ray spectra showed that the 608-, 278-, 377-, 663-, 184-, and 479-keV γ rays all had delayed components. With the time differential measurements, the 184- and 663-keV γ rays were observed to have no prompt component, indicating that the 888-keV state is isomeric. It was also observed that the delayed 278- and 377-keV transitions, which cascade to the 888-keV isomer, had prompt components in their time spectra. This indicated the existence of a second isomeric state lying above the 1543-keV level. However, the 608-keV γ ray, which was the only delayed transition observed to lie above the 1543-keV level, had insufficient intensity in its delayed component to account for the delayed intensity of the 278- and 377-keV γ rays. This implied that the isomeric state responsible for the delayed components of the 278- and 377-keV γ rays decays via a highly converted unobserved transition. The energy of this transition is expected to be less than 95 keV and is denoted by Δ in the level scheme (see Fig. 6). Regarding a third isomeric state, the prompt component observed for the 608-keV γ ray indicates that this isomer lies above the $(2151+\Delta)$-keV level.

With time differential measurements, the mean lifetimes of the $(1543+\Delta)$- and 888-keV isomers were observed to be $\tau=54(2)$ and 28(1) nsec, respectively (see Table II). In addition the weakly populated isomer above $(2151+\Delta)$ keV was found to have a mean lifetime $\tau=82(15)$ nsec. The lifetime of the $(1543+\Delta)$-keV state was determined by a least squares fit of a single lifetime to the spectra of the 278- and 377-keV γ rays. The data for the 278-keV γ ray are shown on the top of Fig. 3; the solid line is the result of the least squares fit to the data which yielded $\tau=54(2)$ nsec. Contributions to the 278- and 377-keV lifetime data from the higher lying isomer above $(2151+\Delta)$ keV were very weak and could be neglected in the analysis. The lifetime of the 888-keV isomeric state was determined from the time differential data of the 663-keV γ ray (see the bottom of Fig. 3). Because this state is also strongly fed by the $(1543+\Delta)$-keV isomer ($\tau=54$ nsec), the data were fitted to the two-lifetime function discussed in Sec. II. The least squares fit to the data yielded $\tau=28(1)$ nsec for the 888-keV isomer. In addition, the fit also yielded 54(4) nsec for the $(1543+\Delta)$-keV isomer which is in excellent agreement with the 54(2) nsec obtained from the 278- and 377-keV time differential data. The lifetime of the isomeric state above the $(2151+\Delta)$-keV level was determined by fitting a single lifetime to the time differential data of the 608-keV γ ray. The fit yielded $\tau=82(15)$ nsec for this isomer. For the remaining levels in ^{212}At, the pulsed-beam-γ timing data yielded mean lifetime upper limits of $\tau\leq 5$ nsec.

The results of the g-factor measurements are summarized in Table II. The uncorrected g factors of the $(1543+\Delta)$- and 888-keV isomeric states were measured to be 0.619(4) and 0.538(8), respectively. The g factor of the $(1543+\Delta)$-keV

TABLE II. Lifetime and g-factor results for ^{212}At.

Energy level (keV)	888	1543 + Δ
J^{π}	(11^+)	(15^-)
τ (nsec)	28 ± 1	54 ± 2
g_{uncorr}	0.538(8)	0.619(4)
g_{corr} [a]	0.541(11)	0.622(10)
g_{calc}	0.61	0.55
E_{γ} (keV)	662.5	183.9
$J_i \rightarrow J_f$	$(11^+) \rightarrow (9^-)$	$(11^+) \rightarrow (10^-)$
α [b]	0.178(8)	0.105(5)
BR [c]	0.63(9)	0.37(5)
$B(\sigma L)$	$B(M2) = 11.1(7)\mu_N^2$ fm^2	$B(E1) = 1.21(12) \times 10^{-6}$ e^2 fm^2

[a] Corrected for diamagnetism and Knight shift; see text.
[b] These values are taken from *Internal Conversion Coefficients*, edited by K. Way (Academic, New York, 1973).
[c] Branching ratios.

isomer was obtained from the perturbed time spectra of the 278-keV γ ray. These data were analyzed to form the ratio $R(t)$ described in Sec. II. The 36 MeV data are shown in Fig. 4 along with the results of a least squares fit which yielded $g = 0.618(9)$. The weighted average of the 36 and 42 MeV data yielded $g = 0.619(4)$ for the g factor of the $(1543 + \Delta)$-keV isomer. The influence of the higher lying isomer at or above

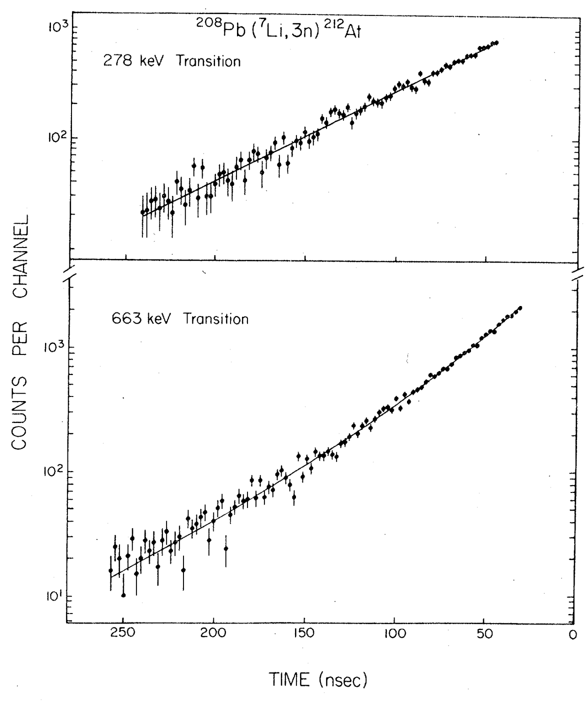

FIG. 3. Results of the time-differential lifetime measurements of the (15^-) and (11^+) states in ^{212}At obtained from the time spectra of the 278- and 663-keV γ rays, respectively. The solid lines are the least squares fits to the data which yielded mean lifetimes of $\tau = 54 \pm 2$ and 28 ± 1 nsec for the (15^-) and (11^+) states, respectively.

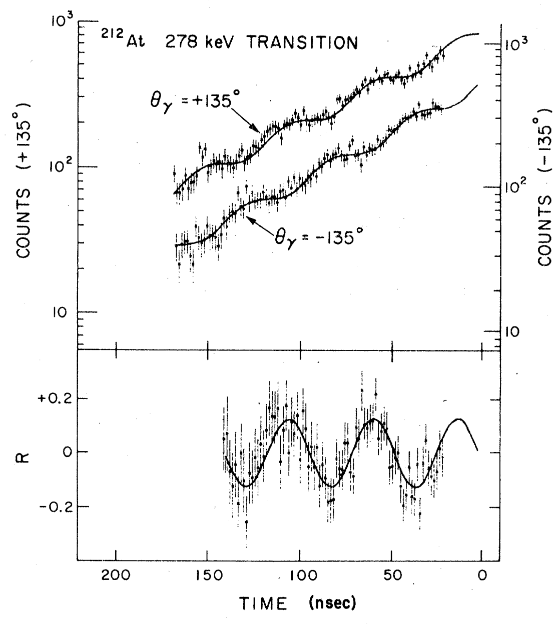

FIG. 4. The results of the perturbed angular distribution measurements of the (15^-) state in ^{212}At obtained with the 278.1-keV γ ray for a ^{7}Li beam energy of 36 MeV. The upper part of the figure is the modulated time spectra obtained with an applied magnetic field of 2.29 T and two Ge(Li) detectors at ±135° to the beam. The lower part of the figure is the ratio R. The uncorrected g factor was found to be 0.619 ± 0.004.

$(2151+\Delta)$-keV on the ratio data for the 278-keV γ ray was found to be negligible. The g factor of the 888-keV isomeric state was determined from the perturbed time spectra of the 663-keV γ ray (see Fig. 5). To extract the g factor of the 888-keV isomeric state, the g factor and lifetime obtained for the $(1543+\Delta)$-keV isomer were inserted as fixed parameters into the two level expression of Ref. 7, which takes into consideration the feeding of the 888-keV level by the $(1543+\Delta)$-keV level. Using this fitting procedure, the g factor of the 888-keV isomeric state was determined from the weighted average of the 36 and 42 MeV data to be $g=0.538(8)$. Estimated corrections[9] to the g factors for diamagnetism and the Knight shift increase the values to $g=0.541(11)$ and $g=0.622(10)$ for the 888- and $(1543+\Delta)$-keV levels, respectively.

The deduced γ-ray multipolarities and J^π assignments for ^{212}At are included in the level scheme in Fig. 6. These assignments were obtained from the angular distributions with the assumptions that the states are aligned in low-m substates and that the dominant γ decay proceeds via yrast levels by stretched transitions $J \rightarrow J-L$ where L refers to the γ-ray multipolarity. Lifetime information and conversion coefficients extracted from delayed γ-ray intensities aided in these assignments. The J^π assignments are also based upon the assumption that the γ-ray cascade ends at the (9^-) 225-keV metastable state.

Although there is no direct experimental evidence that the γ cascade in ^{212}At ends at the 225-keV (9^-) metastable state, the yrast nature of the dominant decay cascade, shown on the right in Fig. 6, and systematics of Li induced fusion-evaporation reactions strongly support this assumption. The γ rays in this cascade decrease in intensity as the energy of the initial state increases. This feature, which is characteristic of the population of yrast levels and the subsequent $J \rightarrow J-L$ stretched γ-ray transitions, is expected in (HI, xn) fusion-evaporation reactions.[2] Since previous studies[4] with Li induced fusion-evaporation reactions have shown that states as high as $15\hbar$ are populated strongly at Li beam energies of about 33 MeV, then in ^{212}At it is also expected that states up to $15\hbar$ are populated. Consequently, the stretched γ-ray decay in ^{212}At will proceed along the yrast line to the 225-keV (9^-) metastable state, which then α-decays to ^{208}Bi. The alternative, that the stretched γ-ray cascade ends at the (1^-) ground state, would indicate that only states up to about $7\hbar$ are populated strongly, which is unlikely in view of the empirical information available for Li beams.

With the assumption that the γ cascade ends at

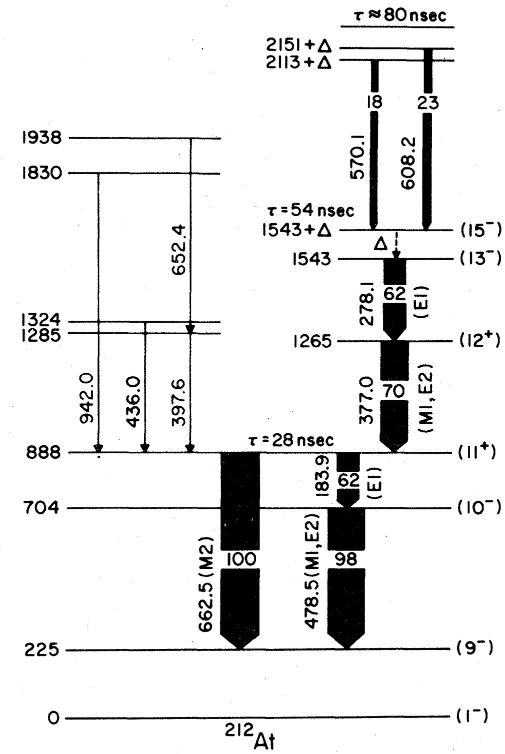

FIG. 6. The energy level scheme of ^{212}At determined from this experiment. The excitation energy in keV is shown at the left and spin-parity assignments at the right. The observed intensities are shown on the transition arrows for the γ rays belonging to the yrast cascade.

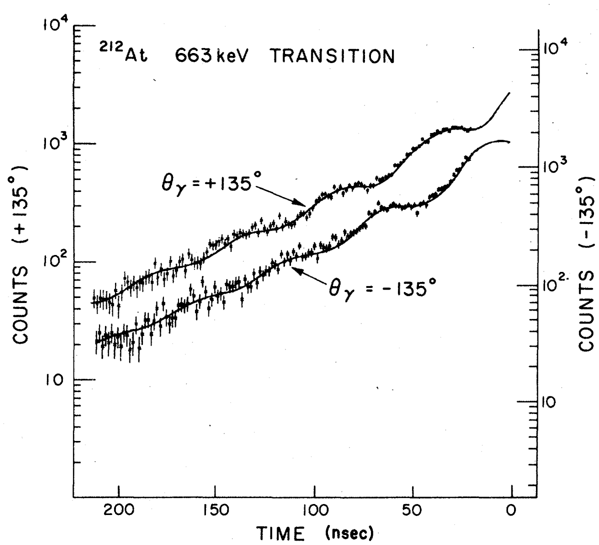

FIG. 5. The results of the perturbed angular distribution measurement of the 888-keV (11^+) state in ^{212}At for a beam energy of 36 MeV. The uncorrected g factor was found to be 0.538 ± 0.008.

the (9^-) 225-keV metastable state, the J^π assignments for ^{212}At were deduced. First consider the yrast cascade on the right side of Fig. 6. The large positive $A_2 = 0.30$ and small negative $A_4 = -0.02$ identified the 663-keV γ ray as a stretched $J \to J-2$ quadrupole transition. The observed mean lifetime $\tau = 28$ nsec suggests an $M2$ multipolarity for this γ ray (an $E2$ transition would be hindered by a factor 10^3 relative to the Weisskopf estimate). Based on the (9^-) 225-keV metastable state, this result implies a J^π assignment of (11^+) for the 888-keV isomeric state. The brackets denote the uncertainty in these assignments. For the 184-, 278-, and 377-keV γ rays, the negative A_2 coefficients imply dipole components for these transitions. A dipole-quadrupole admixture for the 479-keV γ ray is implied by its reduced A_2 coefficient. With the additional lifetime limits and internal conversion coefficients estimated from the delayed γ-ray intensities, the implied multipolarities of the 184-, 278-, 377-, and 479-keV γ rays are $E1$, $E1$, $M1/E2$, and $M1/E2$, respectively. Based on the (9^-) 225-keV metastable state, these multipolarities imply J^π assignments of (10^-), (11^+), (12^+), and (13^-) for the 704-, 888-, 1265-, and 1543-keV levels, respectively. Notice that the γ-ray multipolarities for both branches from the 888-keV isomeric state imply a J^π assignment of (11^+) for this state. For the unobserved transition Δ ($E < 95$ keV), the lifetime $\tau = 54$ nsec is consistent with the Weisskopf estimate for an $E2$ transition between 20 and 95 keV. This suggests a $J^\pi = (15^-)$ assignment for the ($1543 + \Delta$)-keV isomeric state.

IV. DISCUSSION

The experimental results obtained for ^{212}At from the present ^{208}Pb(^{7}Li, $3n$) γ-ray measurements are summarized in Fig. 6 and Tables I and II. The structures of these low-lying high-spin states are expected to be comprised of three protons distributed in the $h_{9/2}$, $f_{7/2}$, and $i_{13/2}$ orbitals and one neutron in the $g_{9/2}$, $i_{11/2}$, or $j_{15/2}$ orbit outside the closed ^{208}Pb core ($Z = 82$, $N = 126$). In particular, these high-spin states are expected to arise from the coupling of the three-proton yrast levels in ^{211}At to the odd neutron. For those ^{212}At states that have primarily a seniority one proton structure, an alternate, but structurally identical view may be taken, namely, these states may be thought of as similar to levels in ^{210}Bi. A comparison of the experimental ^{212}At level scheme with the known ^{210}Bi (Ref. 10) and ^{211}At (Ref. 11) levels suggests the following configurations as dominant components for several of the observed states in ^{212}At:

0-keV (1^-) – $(\pi h_{9/2}{}^3)\frac{9}{2}^- \otimes (\nu g_{9/2})$,

225-keV(9^-) – $(\pi h_{9/2}{}^3)\frac{9}{2}^- \otimes (\nu g_{9/2})$,

704-keV(10^-) – $(\pi h_{9/2}{}^3)\frac{9}{2}^- \otimes (\nu i_{11/2})$,

888-keV (11^+) – $(\pi h_{9/2}{}^2)0^+(\pi i_{13/2}) \otimes (\nu g_{9/2})$,

1265-keV (12^+) – $(\pi h_{9/2}{}^3)\frac{9}{2}^- \otimes (\nu j_{15/2})$,

1543-keV(13^-) – $(\pi h_{9/2}{}^3)\frac{17}{2}^- \otimes (\nu g_{9/2})$,

and

($1543 + \Delta$)-keV (15^-) – $(\pi h_{9/2}{}^3)\frac{21}{2}^- \otimes (\nu g_{9/2})$.

No specific configurations are suggested for the remaining levels in ^{212}At on the basis of the comparison.

Complete shell model calculations for ^{212}At, which would require a very large model space, were not available for comparison. However, since several of the observed ^{212}At states were identified as members of the $(\pi h_{9/2}{}^3)$ $(\nu g_{9/2})$ configuration, a shell model calculation of the energies of this structure was made. This calculation which employed empirical two body matrix elements extracted from ^{210}Bi and ^{211}At yielded the following theoretical energies of 0, 202, 1539, and 1607 keV for the 1^-, 9^-, 13^-, and 15^- states, respectively. The good agreement between the calculated and observed energies indicates a very pure structure for these states. On the basis of this calculation, the yrast $J = 10$, 11, and 12 states are expected at 1247, 1298, and 1506 keV, respectively. Since the observed yrast $J = 10$, 11, and 12 states are located at lower energies, the conclusion can be drawn, that the observed yrast states involve significant components of configurations different from $(\pi h_{9/2}{}^3)$ $(\nu g_{9/2})$. This conclusion is consistent with the above predictions made for these states. In addition, the energy of the $[(\pi h_{9/2}{}^2)0^+(\pi i_{13/2})(\nu g_{9/2})]11^+$ state has been calculated[12] to be 940-keV which is within 52 keV of the measured value.

The electromagnetic properties of ^{212}At give a further test of the nuclear wave functions. The measured g factors for the 888-keV (11^+) and ($1543) + \Delta$)-keV(15^-) states can be compared with those expected for the $[(\pi h_{9/2}{}^2)0^+(\pi i_{13/2})(\nu g_{9/2})]11^+$ and $[(\pi h_{9/2}{}^3)\frac{21}{2}^-(\nu g_{9/2})]15^-$ configurations, respectively. (See Table II.) The additivity property for the effective magnetic moment operator implies that $\mu[^{212}\text{At}(11^+)] = \mu(\pi i_{13/2}) + \mu(\nu g_{9/2})$ and $\mu[^{212}\text{At}(15^-)] = \mu[(\pi h_{9/2}{}^3)\frac{21}{2}^-] + \mu(\nu g_{9/2})$. Using $g(\pi i_{13/2}) = 1.24$ extracted from ^{210}Po,[13] $g(\pi h_{9/2}{}^3) = 0.917$ extracted from ^{211}At,[9] and $g(\nu g_{9/2}) = -0.296$ extracted from ^{210}Bi,[14] the additivity relation predicts $g(11^+) = 0.61$ and $g(15^-) = 0.55$. Although these predictions deviate from the measured values by +13% and −11%, respectively, they show that these configurations are indeed dominant. Since the empirical g factors include core polarization and mesonic effects to the first order, the majority of these deviations are expected to arise from admixtures in the wave functions. Possible admixtures will be discussed below.

A further test of the (11^+) wave function as well as those for the (9^-) and (10^-) levels is provided by the measured $B(M2)[11^+ \to 9^-]$ and $B(E1)[11^+ \to 10^-]$ transition probabilities. The measured $B(M2)$ is compared with that expected for the transition from the $[(\pi h_{9/2}{}^2)0^+(\pi i_{13/2})(\nu g_{9/2})]11^+$ level to the $[(\pi h_{9/2}{}^3)\frac{9}{2}^-(\nu g_{9/2})]9^-$ level. Using the empirical $M2$ transition matrix element extracted from the 1.608-MeV γ ray in ^{209}Bi[15], which is expected to be a primarily a $i_{13/2} \to h_{9/2}$ single proton transition, the $B(M2)$ is calculated to be $12 \pm 8\mu_N^2 \text{fm}^2$. The agreement between this value and the value of $11.1(7)\mu_N^2$ fm^2 obtained from the measured lifetime indicates that the $11^+ \to 9^-$ 663-keV γ ray ^{212}At is predominantly a single proton transition from the $i_{13/2}$ orbit to the $h_{9/2}$ orbit as obtained from the above configurations.

It is interesting to make this comparison with the free nucleon single particle transition $B(M2)$. With a mean radius of $\langle r\rangle = 6.22$ fm obtained from harmonic oscillator wave functions with $\hbar\omega = 41A^{-1/3}$, the $B(M2)$ is calculated to be $93.5\mu_N^2 \text{fm}^2$. The difference between this value and the value of $12\mu_N^2$ fm^2 obtained with the empirical $M2$ matrix element arises predominantly from core polarization effects which are included in the empirical $B(M2)$. Thus the difference between the free nucleon and the experimental $B(M2)$ values does not necessarily imply significant admixtures.

The measured $B(E1) = 1.21\times 10^{-6}\ e^2\text{fm}^2$, which is hindered by a factor of 10^7 relative to the Weisskopf estimates, indicates that the $11^+ \to 10^-$ 184-keV transition is very weak, involving perhaps several small admixtures. This conclusion is supported by the expected $[(\pi h_{9/2}{}^2)0^+(\pi i_{13/2})(\nu g_{9/2})]11^+$ and $[(\pi h_{9/2}{}^3)\frac{9}{2}^-(\nu i_{11/2})]10^-$ configurations between which no $E1$ transition is allowed.

The deviations between the measured and calculated electromagnetic matrix elements in the above discussions imply the existence of admixtures in the (11^+) and (15^-) wave functions. For the 11^+ state, these admixtures are expected to include the $(\pi h_{9/2}{}^3)\frac{9}{2}^-(\nu j_{15/2})$, $(\pi h_{9/2}{}^2)0^+(\pi f_{7/2})(\nu j_{15/2})$, and $(\pi h_{9/2}{}^2)0^+(\pi i_{13/2})(\nu i_{11/2})$ configurations. For the two particle nucleus ^{210}Bi, the calculations by Kuo and Herling[16] show that these configurations have significant amplitudes in the yrast 11^+ wave function. For the (15^-) state, the most likely admixture is the $(\pi h_{9/2}{}^2)(\pi f_{7/2})(\nu g_{9/2})$ configuration, which is expected near 1700 keV.

Finally, it is interesting to extend the comparison between ^{211}At (Ref. 11) and ^{212}At level schemes to levels higher than the $(1543+\Delta)$-keV (15^-) state in ^{212}At. Based on this comparison, it is expected that the $[(\pi h_{9/2}{}^2)(\pi f_{7/2})(\nu g_{9/2})]16^-$ and $[(\pi h_{9/2}{}^2)(\pi i_{13/2})(\nu g_{9/2})]J$, $J = 17^+$ and 19^+, levels should be yrast, with the 19^+ being an isomer with a mean lifetime of about 100 nsec. The present ^{212}At level scheme does not exclude this possibility. According to Blomqvist[12] the 16^- level should be within 100 keV of the 15^- level, thus it would most likely be unobserved. With this assumption it is possible that 608-keV γ ray (see Fig. 6) is the $17^+ \to 16^-$ transition, and the $19^+ \to 16^-$ $E3$ transition is not observed because the isomeric state is populated weakly and the branch for this γ ray could be small. However, according to Blomqvist[12] the 17^+ should be nonyrast, making the 19^+ level an isomer with a mean lifetime of about 14 μsec. No evidence of such a long lifetime was observed in this study.

In conclusion, the structure of high-spin states in ^{212}At has been investigated via in-beam γ-ray spectroscopy with the ^{208}Pb(^{7}Li, $3n$) reaction. As a result, a level scheme involving high-spin states has been deduced for ^{212}At, and several electromagnetic moments have been measured. Comparison of these results with the ^{211}At and ^{210}Bi level schemes and the energies of the $(\pi h_{9/2})^3(\nu g_{9/2})$ configuration has provided a means of identification of the yrast states. However, the experimental matrix elements, namely, the lifetimes and g factors, have shown the complexity of these high spin states. It is clear that to understand these results in a more complete way, larger model-space calculations are essential.

The authors acknowledge Professor J. Blomqvist and Dr. B. A. Brown for contributions which aided in the theoretical interpretation of the experimental results. This study was supported in part by the National Science Foundation.

---

*Present address: Indiana University Cyclotron Facility, Bloomington, Ind. 47405.

†Present address: Cyclotron Institute, Texas A & M University, College Station, Tex. 77843.

‡Present address: Oak Ridge National Laboratory, Oak Ridge, Tenn. 37830.

[1]Paul L. Reeder, Phys. Rev. C 1, 721 (1970); W. B. Jones, Phys. Rev. 130, 2042 (1963).

[2]J. O. Newton, in *Nuclear Spectroscopy and Reactions, Part C*, edited by J. Cerny (Academic, New York, 1974), p. 185.
[3]T. P. Sjoreen, U. Garg, D. M. Gordon, B. A. Brown, and D. B. Fossan, Bull. Am. Phys. Soc. 21, 97 (1976).
[4]T. P. Sjoreen, G. Schatz, S. K. Bhattacherjee, B. A. Brown, D. B. Fossan, and P. M. S. Lesser, Phys. Rev. C 14, 1023 (1976).
[5]O. Häusser, T. K. Alexander, J. R. Beene, E. D. Earle, A. B. McDonald, F. C. Khanna, and I. S. Towner, Nucl. Phys. A273, 253 (1976).
[6]E. Recknagel, in *Nuclear Spectroscopy and Reactions, Part C* (see Ref. 2) p. 93.
[7]R. Lutter, O. Häusser, D. J. Donahue, R. L. Hershberger, F. Riess, H. Bohn, T. Faestermann, F. v. Feilitzsch, and K. E. G. Löbner, Nucl. Phys. A229, 230 (1974).
[8]T. P. Sjoreen, U. Garg, and D. B. Fossan (unpublished).
[9]H. Ingwersen, W. Klinger, G. Schatz, and W. Witthuhn, Phys. Rev. C 11, 243 (1975).
[10]W. W. Daehnick, M. J. Spisak, R. M. DelVecchio, and W. Oelert, Phys. Rev. C 15, 594 (1977); D. Proetel, F. Riess, E. Grosse, R. Ley, M. R. Maier, and P. von Brentano, *ibid.* 7, 2137 (1973) and references therein.
[11]K. H. Maier, J. R. Leigh, F. Puhlhofer, and R. M. Diamond, Phys. Lett. 35B, 401 (1971).
[12]J. Blomqvist, private communication.
[13]T. Yamazaki, T. Nomura, S. Nagamiya, and T. Katou, Phys. Rev. Lett. 25, 547 (1970).
[14]C. V. K. Baba, T. Faestermann, D. B. Fossan, and D. Proetel, Phys. Rev. Lett. 29, 496 (1972).
[15]A. Bohr and B. R. Mottelson, *Nuclear Structure* (Benjamin, Reading, Mass., 1975), Vol. II, p. 565.
[16]T. T. S. Kuo and G. H. Herling, NRL Report No. 2258, 1971 (unpublished).